Wind Stress and Surface Waves Observed on Lake Washington

SERHAD S. ATAKTÜRK AND KRISTINA B. KATSAROS

Department of Atmospheric Sciences, University of Washington, Seattle, Washington

(Manuscript received 23 July 1997, in final form 5 February 1998)

ABSTRACT

New results from turbulent flux measurements made over Lake Washington include the following:

1) The only direct measure of the vertical transport of the horizontal momentum, heat, and matter in the surface boundary layer is the so-called eddy correlation method. However, even if the measurement errors are negligible, the results obtained from point observations may show large scatter due to lack of stationarity and horizontal homogeneity in the turbulent field and to the sampling variability. Scatter may be greatly reduced by spatial averaging. In this study, such an effect is achieved by determining the surface roughness length, hence the neutral drag coefficient, from the measured wave height spectrum, which reflects the atmospheric input integrated over the fetch. Applicability and usefulness of the approach for general field measurements and remote sensing is discussed.

2) The evolution of the wave field observed on Lake Washington agrees in peak frequency and the slope of the equilibrium range parameter α as a function of ''wind forcing'' with other observations, while the magnitude of α is significantly smaller (by a factor of 2.1) than the values obtained from larger bodies of water. Based on the results obtained from a wave model, we attribute this observed difference to the narrower width of the water body on Lake Washington. These findings indicate that the state-of-the-art spectral parameterization of surface waves has limitations in describing the observations from a natural but small body of water.

1. Introduction

Surface fluxes of momentum τ, sensible heat H, and latent heat E can be directly determined by the eddy correlation technique (Busch 1973),

$$\tau = -\rho\overline{u'w'}$$
$$H = \rho C_p\overline{w'T'}$$
$$E = \rho L_e\overline{w'q'}, \quad (1)$$

where u', w', T', and q' are the turbulent fluctuations of horizontal and vertical components of wind, air temperature, and specific humidity, respectively, ρ is the air density, C_p is the specific heat of air at constant pressure, and L_e is the latent heat of evaporation; the overbars denote a space average. One often applies the ergodicity principle, which assumes that stationarity is achieved over a long enough averaging time such that a time average is equivalent to a space average.

Direct measurements of surface fluxes of momentum, heat, and mass are difficult to obtain and in general are not available. An attractive alternative is to estimate them from routinely measured mean quantities, namely the bulk aerodynamic method. However, despite the considerable efforts of many investigators, such parameterization of surface fluxes is not complete. The present paper deals with this issue in the case of momentum flux. Background information is provided in section 2. The field experiment for this study and methods of data processing are described in section 3. In section 4, the experimental findings are presented and discussed. Conclusions are summarized in section 5.

2. Atmospheric surface layer

In the atmospheric boundary layer, the turbulent fluxes of momentum, sensible heat, and latent heat monotonically decrease with height (e.g., Busch 1973). The variation with height is gradual and the fluxes are still within about 10% of their surface values up to a height, say $z < 0.1h$, where h is the height of the boundary layer. The uncertainty in measurements of fluxes with present techniques is also about the same order of magnitude, that is, 10%. Therefore, in this so-called surface layer, the fluxes are considered constant. [See, however, discussion by Donelan (1990) on the systematic error introduced by this assumption.] In this section, the conventional methods of studying the dynamics of the surface layer and formulations of some surface layer parameters are outlined.

Corresponding author address: Dr. Kristina B. Katsaros, Atlantic Oceanographic and Meteorological Laboratory, 4301 Rickenbacker Causeway, Miami, FL 33149-1026.
E-mail: katsaros@aoml.noaa.gov

a. Similarity theory and flux–profile relations

Under stationary and horizontally homogeneous conditions, the turbulence structure in the surface layer can be predicted by the Monin–Obukhov (1954) similarity theory. According to this theory, the height-independent fluxes are scaled with the characteristic values of wind speed, temperature, specific humidity, and Obukhov (1946) length;

$$u_* = \left(\frac{\tau}{\rho}\right)^{1/2}; \qquad t_* = -\frac{H}{\rho C_p}u_*^{-1};$$

$$q_* = -\frac{E}{\rho L_e}u_*^{-1}; \qquad L = -\frac{T_v u_*^3}{g\kappa\overline{w'T_v'}}, \tag{2}$$

respectively, where $T_v = T(1 + 0.61q)$ is the virtual temperature in kelvin and $\kappa = 0.40$ (Zhang 1988; Zhang et al. 1988) is the von Kármán constant; L characterizes the height where the mechanical production and the buoyant energy production become equal, but it should be noted that this height is not exactly $z = -L$ (see Businger 1973).

Similarity theory predicts that mean gradients in the surface layer are universal functions of the stratification parameter z/L. For example, the mean gradient of the wind velocity can be expressed as

$$\frac{dU}{dz} = \frac{u_*}{\kappa(z + z_0)}\phi(z/L), \tag{3}$$

where $z_0 \ll z$ is the surface roughness length. Similar expressions can be written for the gradients of temperature and water vapor. Although z_0 has been introduced to prevent the unrealistic case of infinite shear at the surface, $z = 0$, it also can be interpreted as follows. The momentum flux can be expressed (Obukhov 1946; Businger 1973) in terms of the velocity gradient and the eddy transfer coefficient K_m, or the mixing length l, as

$$\tau = \rho K_m\left(\frac{dU}{dz}\right) = \rho l^2\left(\frac{dU}{dz}\right)^2. \tag{4}$$

Here, K_m represents the product of the eddy velocity and the eddy size, and l represents the turbulent length scale, is sometimes assumed to be proportional to the distance from the solid boundary. As the roughness of the solid boundary increases, both the eddy size and the mixing length becomes larger, resulting in higher levels of turbulence; hence, the momentum flux is enhanced. For neutral stratification [$z/L = 0$ and $\phi = 1$; see Equation (6)], comparisons of Eqs. (2)–(4) show that

$$K_m = u_* l = \kappa u_*(z + z_0). \tag{5}$$

Now, the physical meaning of z_0 becomes obvious: it represents the eddy size and the mixing length near the surface; therefore, it is a measure of the effective roughness of the boundary.

The functional relationships between ϕ and the dimensionless height z/L have emerged from a combination of theoretical work and experimental investigations conducted over land surfaces (Paulson 1970; Businger et al. 1971; Monin and Yaglom 1971; Dyer 1974). A commonly used form for wind velocity (e.g., Liu et al. 1979; Large and Pond 1982; Panofsky and Dutton 1984) is given by

$$\phi = 1 + 7z/L, \qquad z/L > 0$$

$$\phi = (1 - 16z/L)^{-1/4}, \qquad z/L < 0. \tag{6}$$

The velocity profile is obtained by integrating the above equations from z_0 to an arbitrary height z:

$$U - U_s = \frac{u_*}{\kappa}\left[\ln\frac{z}{z_0} - \psi(z/L)\right], \tag{7}$$

where U_s is the surface velocity and ψ is the stratification correction function given by

$$\psi = -7z/L, \qquad z/L > 0,$$

$$\psi = 2\ln\left[\frac{1 + X}{2}\right] + \ln\left[\frac{1 + X^2}{2}\right] - 2\tan^{-1}(X) + \frac{\pi}{2}, \qquad z/L < 0, \tag{8}$$

where $X = (1 - 16z/L)^{1/4}$. As mentioned earlier, the equations above are invalid when the requirements of the similarity theory, that is, stationarity and horizontal homogeneity, are not satisfied. Also, they are not applicable very close to the surface where the turbulence is suppressed and the molecular transport through viscosity becomes important.

Over land, the uncertainties in flux–profile relationships are mainly associated with stratification corrections and roughness lengths. Stratification effects are important at low to moderate wind speeds. At high wind speeds, $L \propto u_*^3$ becomes large and, since as $L \to \infty$, $(z/L) \to 0$ and $\psi(0) = 0$, this similarity theory predicts that the atmospheric surface layer can be assumed neutrally stratified. The surface roughness depends on the characteristics of the terrain.

In the marine environment, the uncertainties mentioned above become larger. One of the reasons is that the stratification correction functions have been derived from observations over land where humidity effects are negligible. Over water the effects of humidity on stratification must be considered, particularly in the case where either a cold air outbreak exists or the surface temperature is warm. Over warm water, particularly in the Tropics, the changes in the atmospheric stratification may be due more to the latent heat flux than to the sensible heat flux. Another reason for larger uncertainties is that the surface roughness has a dynamic nature and it varies as the wave field evolves with wind speed, duration, and fetch. The relationship between the characteristic surface roughness and the sea state is not well understood and is a current subject of investigation (see Brown and Liu 1982; Geernaert et al. 1986; Geernaert

and Katsaros 1986; Hsu 1986; Huang et al. 1986; Toba et al. 1990; Donelan 1990; Donelan et al. 1993).

In the presence of waves and currents, the surface is in motion. Hence, the flux–profile relationships may become even less certain due to severe practical constraints on detailed measurements at the surface and to possible influences of wave and current actions on the distributions of the bulk quantities. For example, U_s, which is set to zero over land, is no longer zero at the air–sea interface. Its value is the alongwind component of surface currents, measurements of which may not be available. Also, influence of the water surface waves on the wind profiles may not be negligible (e.g., Hasse et al. 1978). Over breaking waves, the wind stress may be enhanced by as much as 100% (e.g., Banner 1990). In the presence of slicks, the water surface waves are suppressed. Depending on the size and duration, the slicks may affect the air–sea interaction processes. Slicks, however, only exert a significant (measurable) influence on the sea state for wind speeds less than 6 m s^{-1} (Katsaros et al. 1989). Therefore, in the marine surface layer, the flux–profile relationships must be used with caution.

b. Bulk aerodynamic coefficients

In bulk aerodynamic formulation, the momentum flux is related to the difference in mean wind speed between the surface and some height, z, using a dimensionless coefficient, C_D, [see Eq. (2)];

$$\frac{\tau}{\rho} = C_D[U(z) - U_s]^2 = u_*^2. \tag{9}$$

Despite much effort (see Geernaert 1990), parameterizations of C_D, the so-called drag coefficient, is not complete (e.g., Blanc 1985, 1987; Donelan 1990). Using Eq. (7) and (9), the drag coefficient can be expressed as

$$C_D = \kappa^2\left[\ln\frac{z}{z_0} - \psi(z/L)\right]^{-2}. \tag{10}$$

It is seen that C_D is height dependent (unlike the momentum flux in the surface layer) and it is a function of the roughness length and the atmospheric stratification. Therefore, before the bulk transfer coefficients obtained from different experiments can be compared, they must be adjusted to the same reference state. Generally, the reference height is taken as $z = 10$ m above the surface, and the atmospheric stratification effects are adjusted to neutral conditions, $\psi = 0$. Geernaert and Katsaros (1986) indicate that after such adjustments the remaining effects due to stratification are very small. The drag coefficient corresponding to this reference state is calculated according to

$$C_{DN10} = \kappa^2\left[\ln\frac{10}{z_0}\right]^{-2}. \tag{11}$$

A summary of the results reported by a large number of investigators is given by Geernaert (1990). The highlights of these comparisons can be outlined as follows: C_{DN10} shows a clear, mostly linear trend of increase with wind speed. At low wind speeds, $U \simeq 4$ m s^{-1}, all measurements converge to $C_{DN10} \simeq 1 \times 10^{-3}$ with some scatter. However, toward higher wind speeds, the linear trends diverge systematically such that C_{DN10} at a given wind speed is larger for shallow or fetch-limited sites than for deep open oceans. The waves associated with the shallow or fetch-limited sites (being steeper and moving slower relative to the wind) generally present a rougher boundary to the atmosphere. The observed behavior of the drag coefficient, therefore, is believed to indicate the influence of the wave field (e.g., Geernaert et al. 1986; Smith 1988; Donelan et al. 1993). This is in accordance with Eq. (11).

The above arguments indicate that there is a need for parameterization of the water surface roughness for varying stages of the evolution of a wave field. Such parameterization is necessary to obtain more accurate estimates of not only the momentum flux but possibly heat and water vapor fluxes. In addition, more experimental evidence is required to refine the estimated fluxes both at low wind speeds (that prevail over much of the world's oceans) when stratification effects become significant and surface slicks may form to alter the surface roughnesses and during storm conditions when breaking waves and sea spray can dramatically enhance the transfer processes.

c. Characteristic surface roughness of wind waves

Studies of turbulent flows over a rigid surface (e.g., Tennekes and Lumley 1972) have shown that near the surface the turbulence is suppressed and the flow is entirely determined by the viscous shear. This condition is called aerodynamically smooth flow and it occurs when $zu_*/\nu < 5$, where $\nu = 1.4 \times 10^{-5}$ m^2 s^{-1} is the kinematic viscosity of air. In this so-called viscous sublayer, the velocity profile is linear (or exponential if *surface renewal* is considered). Away from the boundary, when $zu_*/\nu > 30$, that is, at large roughness Reynolds number, the viscous effects become negligible, and the total stress is accounted for by the turbulent transfer. In this region the velocity profile is logarithmic. The height at which the asymptotes of the linear and logarithmic velocity profiles intersect, $\delta_\nu = 11.6\nu/u_*$ (Schlichting 1968), is taken as the viscous sublayer thickness. Then, for aerodynamically smooth flow, the virtual origin of the logarithmic profile or the roughness length can be found as (Donelan 1990)

$$z_0 = \frac{0.11\nu}{u_*}; \qquad u_* < 2(\nu g)^{1/3}. \tag{12}$$

The upper bound of the friction velocity in the above equation is approximately $u_* = 0.1$ m s^{-1}, or $U_{N10} \simeq 3$ m s^{-1}. The corresponding thickness of the viscous

sublayer δ_ν is of the order of 1 mm and decreases with increasing u_*.

Laboratory measurements by Kahma and Donelan (1988) showed that the inception wind speed for wave growth is about $u_* \simeq 0.02$ m s^{-1} (or $U_{N10} \simeq 0.4$ m s^{-1}, and the resulting waves that are not visible yet have a characteristic height ($\equiv 4\zeta$, where ζ is the root-mean-square surface deviation) of about 10 μm. Therefore, at such low wind speeds the waves are buried within the viscous sublayer, and the surface roughness length for aerodynamically smooth flow given by Eq. (12) may be appropriate. Similar results have been reported by Kondo et al. (1973).

As u_* increases, the viscous sublayer gets thinner, hence z_0 first decreases; meanwhile the waves evolve with duration and fetch. Consequently, the waves start to penetrate through the viscous sublayer and interact with the outer turbulent flow (e.g., Kondo et al. 1973). Following this transition of the surface from a relatively smooth to a rough state, the roughness length increases. On dimensional grounds, Charnock (1955) suggested that the surface roughness length over fully developed, wind-generated waves can be described by the wind stress, $\tau = \rho u_*^2$, according to

$$z_0 = \frac{\beta u_*^2}{g}, \tag{13}$$

with the Charnock (1958) constant being $\beta = 0.012$. Comparisons by Smith (1988) of the neutral drag coefficients estimated from Eq. (11) with z_0 given by Eq. (12) and (13) and those obtained from measurements over deep, open oceans (Smith 1980; Large and Pond 1981) have shown that the Charnock formula with $\beta = 0.011$ can successfully describe the observed dependence of C_{DN10} on wind speed except at very high winds where it underestimates the measured stress. However, applications of the same approach to other datasets obtained from marine sites with limited fetch or duration (i.e., where the waves can not reach the fully developed or saturated stage) have required the Charnock constant to be an adjustable parameter (Garratt 1977; Wu 1980; Donelan 1982; Geernaert and Katsaros 1986; Geernaert et al. 1986).

In a fully developed wave field, the dominant waves traveling at speeds comparable to the wind velocity receive little direct energy and momentum from the wind (Dobson and Elliott 1978; Snyder et al. 1981; Hsiao and Shemdin 1983; Hasselmann et al. 1986). In accordance with this, Phillips (1977) argued that the wind input is mainly received by the small-scale waves with phase speeds $c < 5u_*$, and the root-mean-square height of these waves is proportional to u_*^2/g. His physical argument, in which the contribution of the dominant waves to z_0 is neglected, leads to the Charnock formula originally suggested on the basis of dimensional analysis. However, characteristics of the small-scale waves depend not only on wind stress but also on surface tension, water temperature (Kahma and Donelan 1988), drift currents (Banner and Phillips 1974), and modulations by the underlying long waves (e.g., Plant 1990). Also, the small-scale waves, being saturated, are in a state of ubiquitous breaking. They are hence all strongly nonlinear. In addition, under the conditions of strong wind forcing and limited fetch or depth, the dominant waves may support a significant portion of the total wind stress. In summary, Eq. (12) and (13) may describe the asymptotic roughness lengths for some special cases only. They cannot predict the variation of the measured wind stress with sea state, fetch, and depth as outlined by Geernaert (1990) and Donelan (1990). Therefore, in search of a more versatile scheme, various extensions of the Charnock relation have been considered.

A general expression for Eq. (13) was first suggested by Stewart (1974):

$$\frac{gz_0}{u_*^2} = f(c_p/u_*), \tag{14}$$

where c_p is the phase speed of dominant waves. Since the parameters defining the wave field and its dependence on wind speed or stress are related, the function on the right-hand side of Eq. (14) can be expressed in various forms. It should be noted that in this dimensionless representation, Eq. (14), u_* appears on both sides. If the other variables are confined in a narrow range, self-correlation of u_* may lead to spurious results (Perrie and Toulany 1990; DeCosmo 1991; Smith et al. 1992).

Particular forms of $f(c_p/u_*)$ reported from different investigations have been reviewed by Toba et al. (1990). Choosing the form proposed by Masuda and Kusaba (1987):

$$\frac{gz_0}{u_*^2} \propto (\omega_p u_*/g)^m, \tag{15}$$

where ω_p is the frequency of dominant waves, and using a collection of field and laboratory data, Toba et al. (1990) suggested $m = -1$ for the value of the exponent (or, $m = -½$ excluding the Bass Straight data, which did not have direct measurements of u_*). A similar result based on dimensional considerations and experimental data had also been reported by Toba (1979) and Toba and Koga (1986). Noting a high correlation between roughness Reynolds number $z_0 u_*/\nu$ and $u_*^2/\nu\omega_p$, they proposed that $z_0 = 0.025 u_*/\omega_p$. When reduced to the above form this finding also suggests $m = -1$. This result implies that surface roughness increases with decreasing wind forcing, u_*/c_p, or in other words, mature waves are aerodynamically rougher than young waves. This conclusion is in contradiction with the well-established fact that the drag coefficient is smaller over open oceans than coastal waters where waves may not generally reach maturity.

Comparing Eq. (13) and (15) it is seen that the re-

lationship originally proposed by Charnock (1955) corresponds to $m = 0$, a result also supported by Wu (1988). As mentioned before, Charnock's relation should be applied to fully developed waves only.

There is ever increasing evidence that surface roughness decreases as the wind waves grow older, that is, m in Eq. (15) is a positive number. Support for $m = 1$ comes from the field (Kawai et al. 1977; Merzi and Graf 1985; Geernaert et al. 1987; Donelan 1990; DeCosmo 1991; Maat et al. 1991; Smith et al. 1992), laboratory (Masuda and Kusaba 1987; Donelan 1990), and theoretical studies (Janssen 1989, 1991, 1992; Jenkins 1992). A relationship between surface roughness, significant wave height, and wave age proposed by Hsu (1974) can be shown to correspond to $m = ½$. This result was based on the joint consideration of various field and laboratory data.

Possible explanations for the discrepancies summarized above are discussed by Donelan et al. (1993). Since the present work closely follows that of Donelan (1990), the basis of his approach is briefly described below.

Among the existing parameterizations of z_0 that include the effects of the water surface waves, the most commonly accepted one (see Huang et al. 1986; Geernaert et al. 1987; Donelan 1990; Geernaert 1990) is that by Kitaigorodskii (1968, 1970). It is based on the suggestion by Kitaigorodskii and Volkov (1965) that in the presence of surface waves the wind profile in a frame moving with the wave phase speed c can be written as

$$U = c - \frac{u_*}{\kappa} \ln\frac{z}{a} = \frac{u_*}{\kappa} \ln\frac{z}{h_s}, \tag{16}$$

where $h_s = a \exp(-\kappa c/u_*)$ and a is some function of wave height. Comparison between Eqs. (7) and (16) shows that $z_0 \propto h_s$, but the nature of the relationship must be determined experimentally (e.g., Geernaert et al. 1986; Huang et al. 1986). Invoking a similar argument, Kitaigorodskii (1968) found that

$$h_s^2 = 2 \int_0^\infty E(k) \exp(-2\kappa c(k)/u_*)\, dk, \tag{17}$$

that is, h_s is the root-mean-square wave height weighted by a function of the wave age c/u_*. Application of this approach requires that the wave energy density spectrum is known over all wavenumber space. However, such measurements may not be available particularly at high wavenumbers, and generally an empirical or theoretical spectral form is adopted. If the latter approach is used, Eq. (17) and other parameterizations that utilize the wave spectra (e.g., Byrne 1982; Donelan 1982) reduce to some generalized form of the Charnock relation (see Kitaigorodskii 1970; Geernaert et al. 1986; Huang et al. 1986).

A simple alternative to Eq. (17) was proposed by Kitaigorodskii (1970): $z_0 = 0.3\zeta \exp(-\kappa c_p/u_*)$. Donelan (1990) noted that this compact formulation of z_0 represents most of the field data quite well, but underestimates near full development due to the exponential dependence on u_*/c_p, the so-called wind forcing. Therefore, modifying the exponential term, he obtained

$$\frac{z_0}{\zeta} = 5.53 \times 10^{-4}\left(\frac{U_c}{c_p}\right)^{2.66} \quad \text{or} \quad \frac{z_0}{\zeta} = 1.84\left(\frac{u_*}{c_p}\right)^{2.53}, \tag{18}$$

where U_c is the component of U_{N10} in the direction of the waves at the spectral peak. Since $\zeta \propto (U_c^2/g) \cdot (U_c/c_p)^{-1.65}$ (Donelan et al. 1985), the above formulation corresponds to Eq. (15) with $m = 1$. The advantage of this approach is that there is no scaling variable that appears on both sides of the equality; hence potential problems due to self-correlations are avoided. On the other hand, in the presence of swell or mixed seas, applicability of Eq. (18) is not straightforward.

The ultimate goal here is to determine the surface roughness length so that surface fluxes can be calculated through the bulk aerodynamic formulae. Equations (15) and (18), although useful for exploring the nature of z_0 cannot be used for this purpose because, in addition to ζ and c_p, they require that u_* or U_{N10} are known. In the present study, the wind forcing term (U_{N10}/c_p or u_*/c_p) in Eq. (18) is replaced by a measurable parameter of the wave field, namely, the equilibrium range parameter α. As shown by Donelan et al. (1985) these two quantities, α and U_{N10}/c_p, are highly correlated. Although evolution of a wave field is a slow process, response of the equilibrium range parameter to varying wind conditions is remarkably fast (Toba et al. 1988). Thus the surface roughness length can be estimated from α determined from measurements of water surface waves alone. Using the field data, success of the approach is demonstrated and its potential is discussed.

3. Experimental setup and data processing

a. Experimental site

The field data used in this study were collected during the summers of 1986–89 at Sand Point, Lake Washington, Seattle (Figure 1a). The research facility is operated by the Air–Sea Interaction Group of the University of Washington, Department of Atmospheric Sciences. It consists of a mast located 15 m offshore (Figure 1b), a hut situated on a beached barge, and a floating dock between the mast and the land. On the beach, the dock is mounted on a rotating base so that the offshore end can swing between the barge and the mast. In order to prevent interference with the measurements, during data acquisition the dock is secured along the shore away from the mast. A data link between the instruments on the mast and the data acquisition system in the hut is supplied by underwater cables. Until the early summer of 1988, the station was powered by a diesel generator. Since then line power has been available.

Ideal experimental conditions at this site are achieved

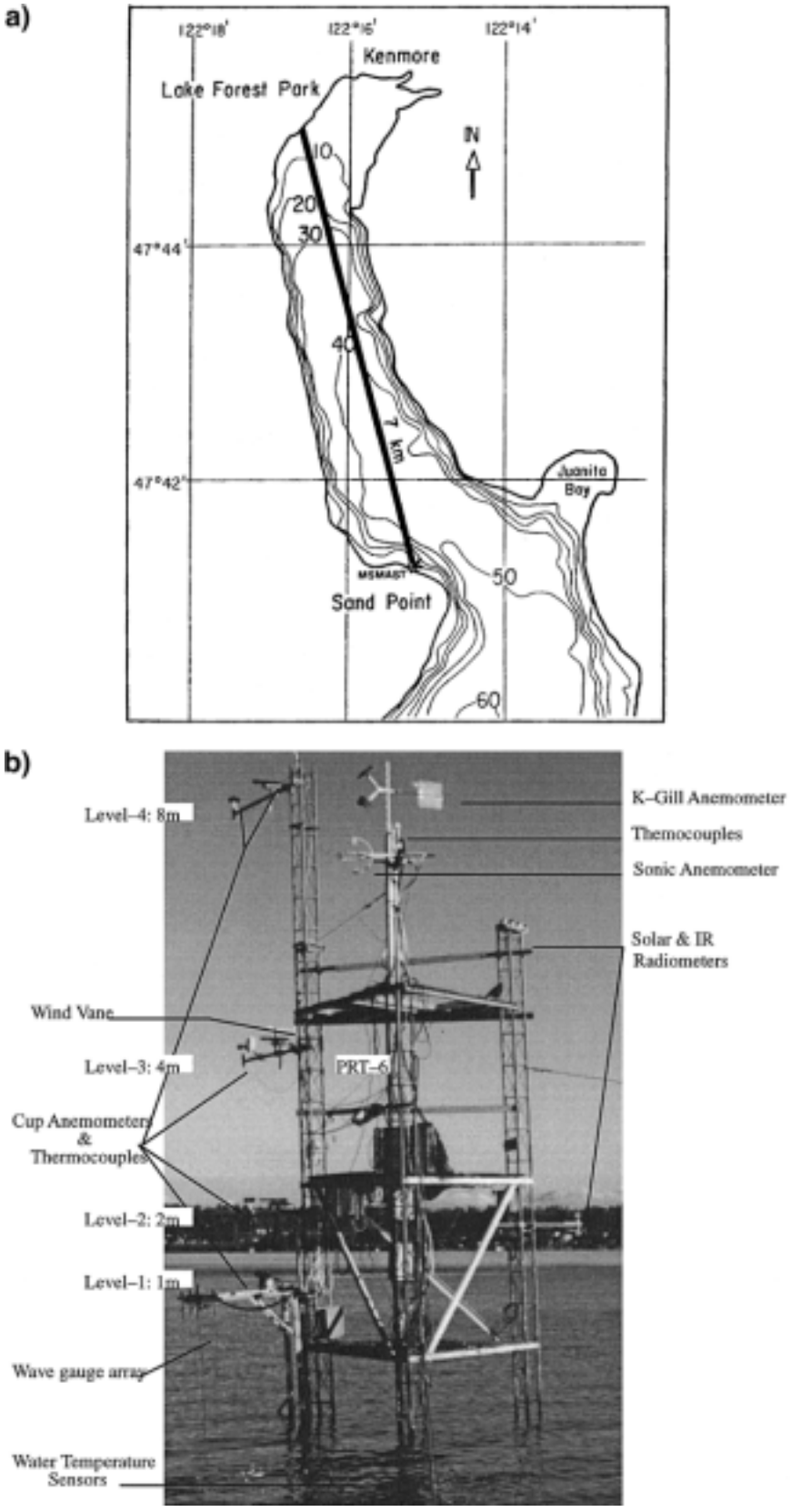
a)
122°18'
122°16'
122°14'
Kenmore
Lake Forest Park
N
10
20
30
47°44'
40
7 km
47°42'
Juanita Bay
MSMAST
50
Sand Point
60
b)
Level–4: 8m
K–Gill Anemometer
Themocouples
Sonic Anemometer
Solar & IR Radiometers
Wind Vane
Level–3: 4m
PRT–6
Cup Anemometers & Thermocouples
Level–2: 2m
Level–1: 1m
Wave gauge array
Water Temperature Sensors

during northerly winds when the fetch over the lake reaches a maximum of about 7 km. The location offers the opportunity to study surface waves generated by the local wind on a natural body of water under a variety of environmental conditions without the complexities that may arise from the presence of swell or tidal currents. The water depth D by the mast is approximately 4 m and increases rapidly farther offshore. We estimate the degree of reflection of the the gravity waves from the inclined beach to be 5% or less (Miche 1951). When $kD > \pi/2$, where k is the wavenumber, the waves are said to be in deep water (Phillips 1977, p. 37). This corresponds to $\lambda = 2\pi < 16$ m, where λ is the wavelength. Since this condition was met in all cases (typically $\lambda \cong 5$ m for the dominant gravity waves), the location can be considered as representative of deep water.

b. Instrumentation

The parameters of interest for the present study were amplitudes of water surface waves, wind speed and stress, water temperature, and atmospheric stratification. Continuous visual records of the water surface were also obtained to identify breaking waves, suppression of surface roughness due to surfactants, and contamination of wave measurements due to boat waves or sea weeds. Only clean-surface cases were included in this study. Acquisition of such complete sets of data was achieved employing several instruments that are described next. (For more detail, see Ataktürk 1991.)

Wave gauge. The water surface elevations were measured using a resistance wire gauge (Ataktürk 1984; Ataktürk and Katsaros 1987). The diameter of the stainless steel wire was 0.13 mm. The resistance of the portion of the wire exposed to the air is a linear function of the water surface elevation, to a very good approximation. However, comparisons with a laser displacement gauge (LDG) in a wave tank by Liu et al. (1982) showed that at high frequencies the dynamic response of the wire gauge to vertical surface displacements was limited. After correcting for the reduced dynamic response, they observed good to excellent agreement between the spectra of the wire data and the LDG data up to 40 Hz.

Propeller–vane anemometers. Wind data were collected at several heights. Low-level observations (0.5–4.0 m above the mean water level) of the wind speed and direction were made by Gill single propeller–vane anemometers (Holmes et al. 1964; Gill 1975). A different type of device, the K–Gill twin propeller–vane anemometer (Ataktürk and Katsaros 1989) was placed at heights ranging from 4.5 to 8.5 m. The K–Gill yields the wind speeds along the axes of its two propellers, one looking up and one looking down at angles of $\pm 45°$. A level sensor attached to the instrument measures the inclination angle of the propellers. In addition to these, the angular response characteristics of the propellers, determined through wind tunnel studies, are required to obtain the vertical and the downstream horizontal components of the wind vector from which the wind stress can be calculated. The method of resolving the wind components employed in this study is described by Ataktürk and Katsaros (1989). Corrections for the angular and frequency responses of the propellers were applied to the time series of these data (Ataktürk 1991).

Intercomparisons of the momentum fluxes measured during HEXMAX (DeCosmo 1991; Smith et al. 1992; DeCosmo et al. 1996) by the K–Gill anemometer and a sonic anemometer showed that K–Gill results were lower by 10%–20%. After corrections to the K–Gill data, in the frequency domain following Hicks (1972), the differences were reduced to 5% or less. The atmospheric stratification during HEXMAX was mostly neutral or slightly unstable. Since the eddies with dimensions smaller than the spacing between the propellers are not resolved, the performance of the K–Gill anemometer is expected to be poorer during stable conditions when a significant portion of the momentum flux may come from small eddies.

Psychrometer. Thermocouples were used to measure the dry-bulb (T_d) and the wet-bulb (T_w) temperatures (e.g., Shaw and Tillman 1980; Katsaros et al. 1994a) in detail. The chromel–constantan sensors were 50 μm in diameter. The wet-bulb sensor was wrapped with cotton thread that was kept moist with a controlled flow of water from a reservoir. A pair of sensors was usually used at a height of 2 m. A second pair was mounted just below the lower propeller of the K–Gill anemometer but far away enough to prevent flow distortion. A thermocouple psychrometer and the K–Gill anemometer together provided the sensible and latent heat fluxes across the air–water interface.

For computation of the surface fluxes from atmospheric turbulence measurements, sensors with a short response time are required. Generally, a bare, fine wire thermocouple, such as the one used in this study to measure the sensible heat flux, meets this requirement. However, when the same thermocouple is used to measure the wet-bulb temperature, its response time may be reduced by a factor of 10 due to the water-soaked wick around it. The specific humidity from which the latent heat flux is calculated, depends on the difference between the dry- and wet-bulb temperatures. Any difference between the dry- and wet-bulb temperatures that may result from unmatched response times of the sen-

←

FIG. 1. (a) The location of our field station (MSMAST) on Lake Washington. The tower is 15 m offshore and at a water depth of 4 m. The contours show the water depth in meters. (b) The Lake Washington tower (photo 1995) with meteorological instrumentation, wire wave gauge, and the video camera. The tower has been designed to minimize the flow distortion and the reflection of waves from the supporting structure. The land in the background is Juanita Bay on the east side of the lake.

sors can cause large errors in the specific humidity and may significantly change the shape of the humidity spectrum (e.g., Shaw and Tillman 1980). In the present study, the frequency responses of the two sensors were matched by speeding up or deconvolving the wet-bulb signal with its frequency response function (e.g., Ataktürk 1991; DeCosmo 1991).

Thermistors. The water temperature was measured using an array of thermistors with average depths of the sensors ranging from 0.30 to 0.80 m below the mean water level. The information from the sensor closest to the surface was used to determine the temperature difference between air and water. The sensors were calibrated in the field using water baths.

Video camera and recorder. Visual records of the fine features on the water surface were made by a Panasonic WV—3110 color video camera and a Panasonic NV—8200 video cassette recorder. The comments by the observer were recorded on the audio channels of both the instrumentation and the video recorders. In this way, the two recorders could be synchronized during playback. The video records were used to identify sections of the data affected by breaking events, boat waves, sea weeds, and surface slicks.

c. Description of the datasets analyzed

Measurements of wave heights and surface fluxes of momentum, sensible heat, and latent heat were analyzed using 79 datasets. Each dataset is approximately one hour long. All observations were made during northerly winds. Average wind speeds, adjusted to 10-m height and neutral atmospheric stratification, were in the range $2 < U_{N10} < 9$ m s^{-1}. Water temperatures near the surface (0.30 m below the mean water level) were mostly between 21° and 24°C, except during May 1987 when it was about 15°C. The differences between the air temperature (at 10-m height) and the water surface temperature varied between approximately +5° and −5°C, indicating that the experimental conditions included all possible cases of atmospheric stratification, that is, unstable, neutral, and stable. The atmospheric stratification parameter z/L, calculated for each dataset, was mostly within the range $-0.7 < z/L < 0.5$, except during very light winds, $U_{N10} \approx 2$ m s^{-1}, when values of $|z/L| > 2$ were found.

In general, the growth stage of the observed wave fields varied from young to relatively mature as measured by the wind forcing parameter $1 < U_{N10}/c_p < 2.5$. Note that the value 2.5 is very large, and difficult to observe in the open sea. In some cases $U_{N10}/c_p < 1$; that is, decaying wave fields were observed during decreasing wind conditions. On 18 May 1987, under the action of relatively strong winds, the wave field reached a state with significant wave height of 0.32 m, spectral peak frequency of 0.45 Hz and a wavelength of about 8 m. At our experimental site, these values may be considered as the extremes during northerly winds. Generally, the significant wave heights do not exceed 0.20 m, and the peak frequency is about 0.55 Hz, corresponding to a wavelength of about 5 m.

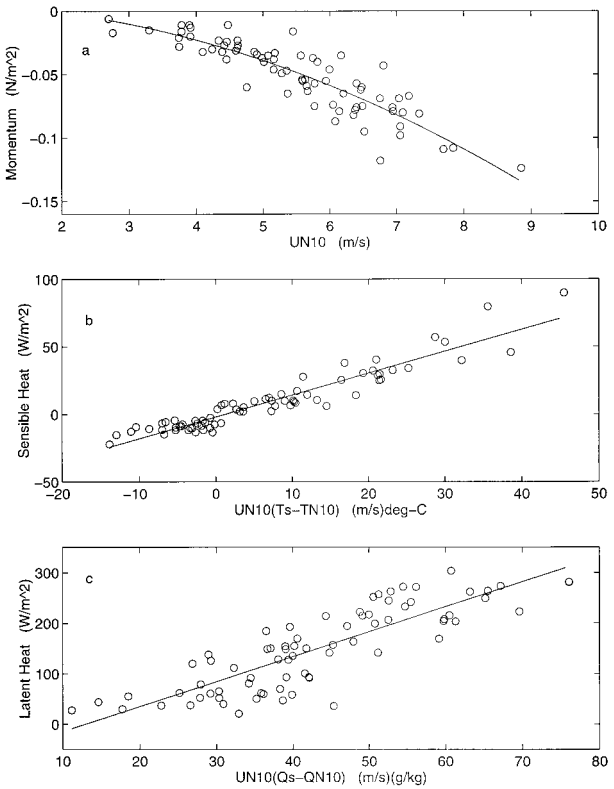

FIG. 2. Magnitudes of surface fluxes measured at MSMAST on Lake Washington by the eddy correlation technique. Solid lines indicate the (a) quadratic or (b, c) linear fits to the datasets. Regression line and the rms error $e_{\rm rms}$ for each plot are (a) $\tau = -\rho[0.14(U_{N10})^2 + 0.44U_{N10} - 1.83] \times 10^{-2}$, $e_{\rm rms} = 0.013$ N m^{-2}; (b) $H = \rho C_p[1.6U_{N10}(T_s - T_{N10}) - 1.8]$, $e_{\rm rms} = 7.0$ W m^{-2}; and (c) $E = \rho L_e\,[5.0U_{N10}(Q_s - Q_{N10}) - 67.0]$, $e_{\rm rms} = 43.7$ W m^{-2}.

4. Experimental findings and discussions

Ranges of surface fluxes and some key parameters encountered in this experimental work are illustrated in Fig. 2. These fluxes were obtained from atmospheric turbulence measurements by using the eddy correlation method. In these plots a positive value for flux indicates upward transfer from water to atmosphere. Cases with *measured* wind speeds less than 3.5 m s^{-1} were discarded due to inadequate frequency response of the instruments under such conditions. Note that in Fig. 2, wind speed, temperature, and specific humidity have been adjusted to neutral atmospheric stratification and 10-m height [Eqs. (2), (7), and (8)]. In the remainder of this manuscript all adjusted parameters are identified by the subscript $N10$. Quadratic dependence of momentum flux on wind speed is depicted by the solid curve in Fig. 2a. Linear regressions (solid lines in Figs. 2b,c) were used for the heat fluxes. For the ranges in-

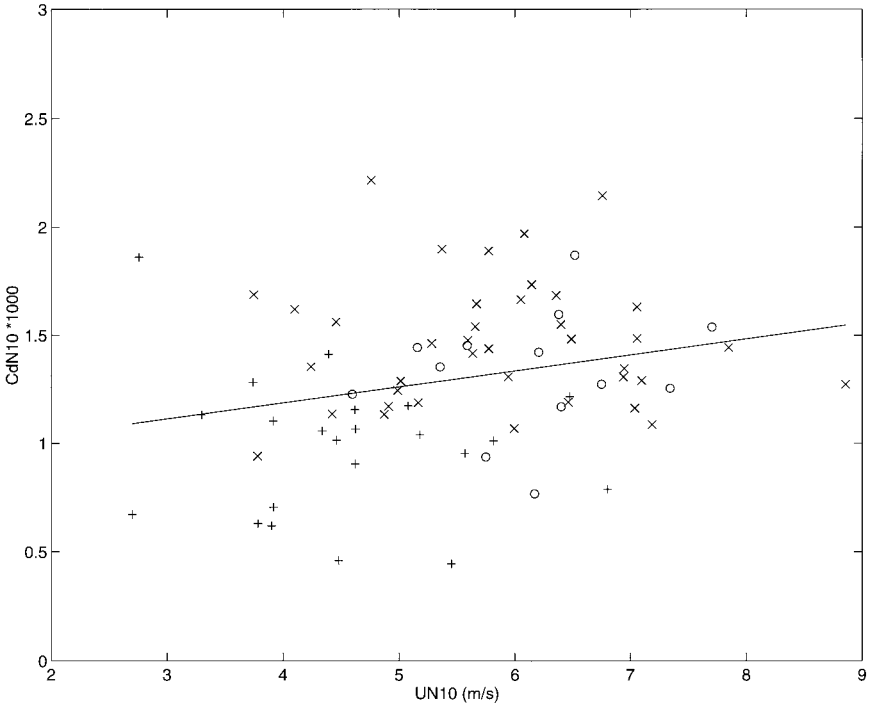

FIG. 3. Neutral drag coefficient, obtained from atmospheric turbulence measurements at MSMAST on Lake Washington, increases with increasing wind speed. Symbols indicate the atmospheric stratification associated with a data point: (×) unstable $z/L < -0.1$, (+) stable $z/L > 0.05$, and (○) near neutral. Linear regression (solid line) and the root-mean-square error e_{rms}, are $C_{dN10} = [0.08U_{N10} + 0.84] \times 10^{-3}$, $e_{\text{rms}} = 0.35 \times 10^{-3}$.

dicated in Fig. 3, regression equation and the root-mean-square error e_{rms} for each fit are

$$\tau = -\rho[-1.8(U_{N10})^2 + 6.0] \times 10^{-3}, \qquad e_{\text{rms}} = 0.013 \text{ N m}^2,$$

$$H = \rho C_p[1.6U_{N10}(T_s - T_{N10}) - 2.0], \qquad e_{\text{rms}} = 7.1 \text{ W m}^2,$$

$$E = \rho L_e[4.9U_{N10}(Q_s - Q_{N10}) - 63.6], \qquad e_{\text{rms}} = 43.1 \text{ W m}^2. \quad (19)$$

Customarily, results from measurements of surface fluxes are reported in terms of bulk transfer coefficients; therefore, that approach is also followed here. In Fig. 3, the drag coefficient is plotted against the wind speed. Different symbols indicate the atmospheric stratification associated with a data point (×: unstable $z/L < -0.1$, +: stable $z/L > 0.05$, and ○: near neutral). In this limited range of wind speeds encountered, the drag coefficient slightly increases with wind speed. Regression equation and the rms error for the plot in Fig. 3 are

$$C_{DN10} = [0.08U_{N10} + 0.84] \times 10^{-3}, \qquad \pm e_{\text{rms}} = 0.35 \times 10^{-3}. \quad (20)$$

In general, magnitude and behavior of the drag coefficient determined in this study are typical of results obtained by others in the marine environment (e.g., Donelan 1990; Geenaert 1990). A remaining dependence of the neutral drag coefficient on stratification may be hinted in Fig. 3 but, considering the weakness of this effect and the scatter in the data, this issue may not be argued convincingly based on this dataset (see also Geernaert and Katsaros 1986).

Equation (11) states that the drag coefficient adjusted to neutral atmospheric stratification and a reference height of 10 m depicted in Fig. 3 depends only on the surface roughness length z_0, that is, the height of the virtual origin of the logarithmic profile of wind speed. Thus, a parameterization of one would readily yield the other. Unfortunately, direct determination of the roughness length through atmospheric turbulence measurements is extremely difficult. Since it varies exponentially with the drag coefficient, the effect of the scatter seen in Fig. 3 becomes much more dramatic. This is illustrated in Fig. 4, where z_0 normalized by the rms wave height ζ is plotted against the wind forcing term U_{N10}/c_p. Also shown are Eq. (18) (Donelan 1990: solid line) and the fit to the HEXMAX dataset (Smith et al. 1992: dashed line). The reason for selecting these particular examples is that both have been obtained from wide ranges of wind and wave conditions and the instrumentation of this work also has been used in the HEXMAX experiment (DeCosmo et al. 1996). De-

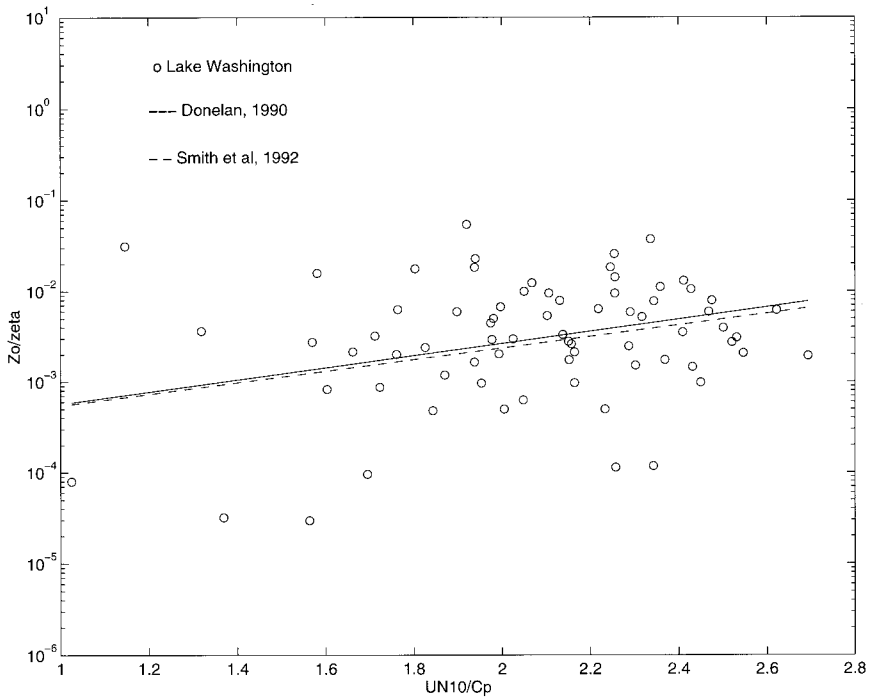

FIG. 4. Surface roughness length normalized by the rms wave height z/ζ versus the wind forcing U_{N10}/c_p, showing that as a wave field matures the surface roughness decreases. The solid line is from Lake Ontario [Donelan 1990; also, Eq. (18)]; the dashed line is from the North Sea data (Smith et al. 1992). Despite the scatter in the Lake Washington dataset, these results are in good agreement and indicate a close relationship between z_0 and the water surface waves.

spite the scatter in the Lake Washington dataset, the agreement between these three studies is obvious, indicating a close relationship between z_0 and the water surface waves.

To improve our current understanding and modeling of the air–sea exchange processes, seeking alternative methods of investigation in addition to traditional ones may prove useful. In light of Fig. 4 and the discussions in section 2c, it seems plausible that information about z_0 may be obtained from parameters of the wave field. Such an attempt is introduced next.

Detailed studies of wind generated waves on Lake Ontario and in the laboratory by Donelan et al. (1985) show that the equilibrium range parameter α, defined as the spectral energy density averaged over the frequency range, $1.5 < \omega/\omega_p < 3.5$, where the spectral slope is -4, plays a key role in describing a wave spectrum. It is also shown that α is highly correlated with the wind forcing term:

$$\alpha = 0.006\left(\frac{\cos\theta U_{N10}}{c_p}\right)^{0.55}; \qquad 0.83 < U_{N10}/c_p < 5, \tag{21}$$

where θ is the angle between the propagation direction of dominant waves and wind. Figure 5 shows the comparison of Eq. (21) with the Lake Washington data where α was calculated over the range; $1.5 < \omega/\omega_p < 3$, since at higher frequencies the spectral slope exceeds -4. Differences in slopes between Eq. (21) and the measurements are insignificant, but systematic deviation of the Lake Washington data in magnitude (by a factor of 2.1, corresponding to a 52% reduction) from the Lake Ontario data is clear (Aktaktürk 1991). This difference implies that for a given wind forcing, the waves on Lake Washington do not grow as large in amplitude as those on Lake Ontario. We have also noted that despite the differences in wave amplitudes, the peak frequencies observed on Lake Washington were in close agreement with the values calculated following Donelan et al. (1985) for the same conditions. These results can have significant implications for air–sea interaction processes, currents, and vertical mixing in the water in coastal seas and estuaries. Results similar to those of Aktaktürk (1991) above were also noted by Kahma and Pettersson (1994) from observations in the Gulf of Finland and the Bothnian Sea. They found that for similar conditions the dimensionless energy at the same peak frequency was 37% larger for the broad fetch than for the narrow fetch, while there was no significant effect of the basin width on the peak frequency. They suggested that the observed difference in the growth of wind waves is due to the dependence of the spectral shape on the basin geometry. We also support this suggestion for the following reason.

Changes in wave spectral energy are described by the radiative energy transfer equation (Hasselmann 1960),

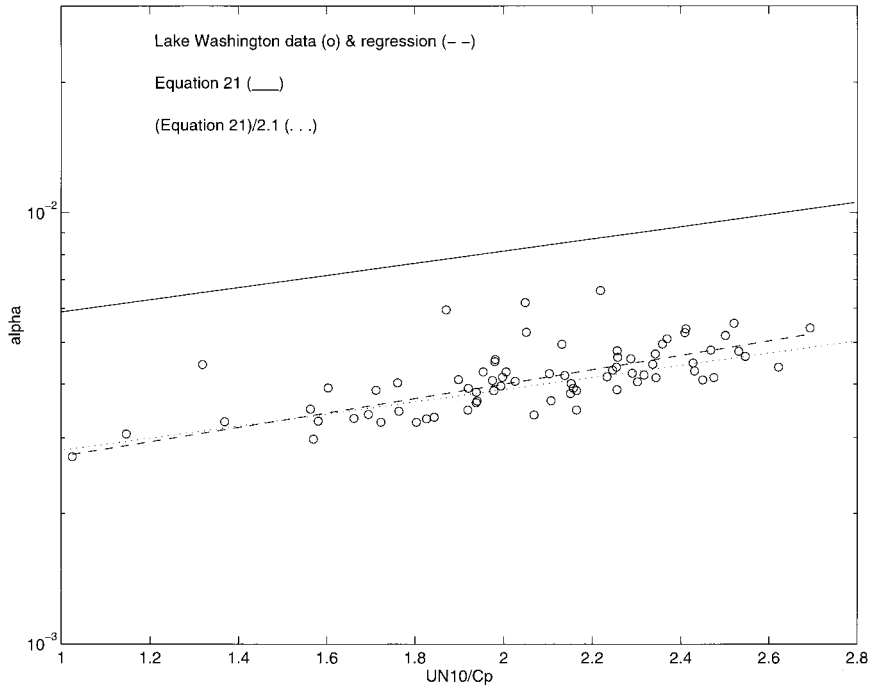

FIG. 5. Equilibrium range parameter α versus wind forcing, showing that results from Lake Washington differ from Eq. (21) (solid line, Donelan et al. 1985) in magnitude by a factor of 2.1 (dotted line), systematically. The difference in slope is insignificant. The fit to Lake Washington dataset is described by Eq. (22) (dashed line).

which involves three source terms: input from wind, dissipation, and the weakly nonlinear wave–wave interactions. The first, and particularly the second term, are poorly known. The nonlinear energy transfer between waves described by the last term (Hasselmann 1962) controls the rate of evolution of a wave spectrum. However, this term strongly depends on the *assumed* spectral shape (Hasselmann et al. 1985). As noted by Ataktürk (1991), the spectral width of the wave spectra observed on Lake Washington is narrower than those observed on Lake Ontario. Therefore, the growth rates of waves from these two sites are also expected to differ. The two sites also differ in that waves on Lake Washington are confined to a narrower angular range, and this difference should have a role in determining the spectral shape. Directional measurements of the wave spectra on Lake Washington are in progress to address this issue.

In order to further test the idea that shorelines are important in that they absorb wave energy, spreading in their directions but not allowing for any energy coming into the region from these directions, a numerical test of the wave growth in a narrow basin was performed. Hans Hersbach of the Royal Dutch Meteorological Institute performed a run with the well-known Community Wave Model (WAM; Komen et al. 1995) using the dimensions of the bay of Lake Washington and postulating absorbing beaches. He compared similar runs with infinite width of the water body. These comparisons showed that (H. Hersbach 1996, personal communication) for wind speeds 4–10 m s^{-1}, the narrow basin of Lake Washington was responsible for 30%–40% reduction in the wave energy or equivalently in the equilibrium range parameter. The tests also indicated a smaller reduction of 5%–10% in downshifting of the spectral peak frequency, which agrees with our observations. This simple test, by explaining a large part (58%–77%) of the difference in the equilibrium range parameters obtained from Lake Washington and Lake Ontario, provides further support to our hypothesis.

Noting that z_0/ζ and α are both closely related to U_{N10}/c_p, one can estimate the surface roughness length from the equilibrium range parameter. In the present study, U_{N10}/c_p is eliminated between

$$\alpha = 0.0027\left(\frac{U_{N10}}{c_p}\right)^{2/3}; \qquad 1.2 < U_{N10}/c_p < 2.6, \quad (22)$$

which is a linear fit to our data set (Fig. 5) and Eq. (18) (Donelan 1990) to obtain

$$z_{0\zeta} = 5.53 \times 10^{-4}\zeta\left(\frac{\alpha_m}{0.0027}\right)^4. \quad (23)$$

The subscripts ζ and m are used to stress that $z_{0\zeta}$ is determined from a parameter of the wave spectrum α_m, as *measured* in Lake Washington. Results from Eq. (23) may be evaluated by plotting $z_{0\zeta}$ against u_*, which is measured independently (Fig. 6). Also shown are z_0

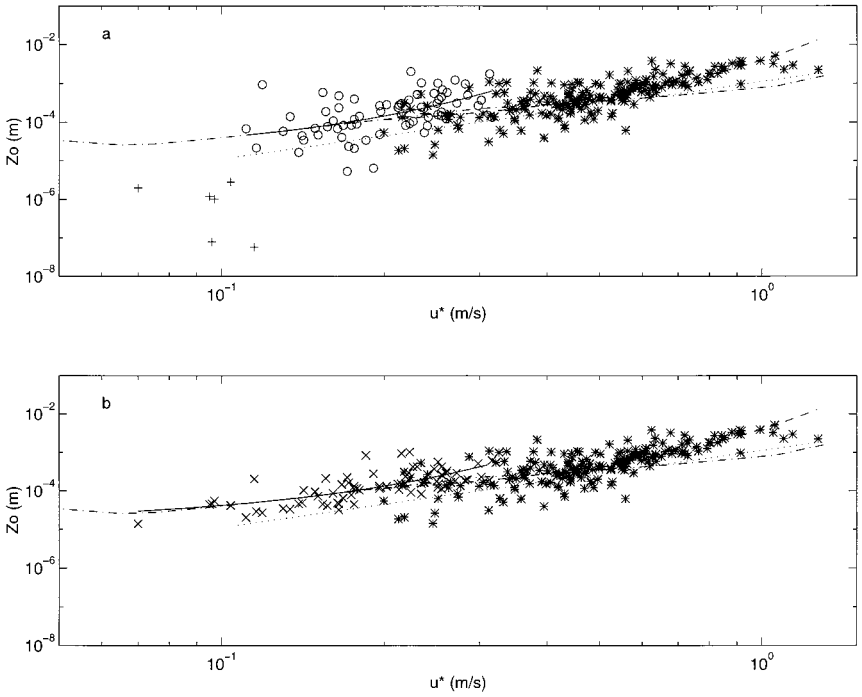

FIG. 6. Surface roughness length z_0 versus friction velocity u_*. Lake Washington data in plots a and b were obtained from measurements of turbulent fluxes (○ and +) and surface waves (×), respectively. Solid lines are from linear regression analyses of these datasets, exclusive of the points marked with + in the upper plot. Both plots also show (i) the HEXMAX results based on turbulent fluxes (*) and a linear fit to the data (· · ·); (ii) the values calculated following Liu et al. (1979) (–·–); and (iii) Eq. (13) with Charnock constant $\beta = 0.011$ (— —). Note that at low u_*, while z_0 from fluxes (plot a, Lake Washington and HEXMAX shows considerable scatter, $z_{0\zeta}$ from waves exhibits a clear and consistent behavior down to the levels of aerodynamically smooth flow. At the lowest values of u_* (where there are no data points) the waves are buried within the viscous sublayer and the roughness length is determined by Eq. 12 as indicated by Liu et al. (1979). Regression line and e_{rms} for the Lake Washington LW and HEXMAX datasets are (a) LW–flux: $\ln z_0 = 13.47u_* - 11.56$, $e_{\text{rms}} = 1.05$; (b) LW–wave: $\ln z_0 = 11.55u_* - 11.23$, $e_{\text{rms}} = 0.64$; and (a, b) HEXMAX–flux: $\ln z_0 = 4.43u_* - 9.95$, $e_{\text{rms}} = 0.75$.

determined from flux measurements on Lake Washington and in the North Sea (DeCosmo 1991), as well as the values calculated following Liu et al. (1979) and from Eq. (13) with the Charnock constant $\beta = 0.011$ (e.g., Smith 1980). As seen in Fig. 6a, z_0 obtained from fluxes measured in the Lake Washington and HEXMAX experiments shows good agreement with the predicted values but with considerable scatter, as expected. Near the low end of the u_* range, several data points (marked with +) from the Lake Washington dataset fall to levels significantly below that given by the Charnock relation. This is contrary to expectations, because the Charnock relation is appropriate for z_0 over open oceans where the roughness length is typically smaller than in coastal waters or lakes. Hence, these points were excluded from statistical analysis. On the other hand, $z_{0\zeta}$ obtained from measurements of the equilibrium range parameter of wave spectra exhibits a consistent behavior throughout the range considered (Fig. 6b). The regression line and e_{rms} for the Lake Washington (LW) and HEXMAX datasets are

$$\begin{aligned} \ln z_0 &= 13.47u_* - 11.56, \\ e_{\text{rms}} &= 1.05 \quad \text{(LW–flux)} \\ \ln z_{0\zeta} &= 11.55u_* - 11.23, \\ e_{\text{rms}} &= 0.64 \quad \text{(LW–wave)} \\ \ln z_0 &= 4.43u_* - 9.95, \\ e_{\text{rms}} &= 0.75 \quad \text{(HEXMAX–flux).} \end{aligned} \tag{24}$$

(The above expressions have been constructed only for the purpose of statistical comparisons and are not suggested for use over water in other sites since they do not include the wave properties.) Equation (24) shows that although the two methods of determining the surface roughness length (LW–flux and LW–wave) lead to similar results, the latter approach has much less scatter as indicated by a 39% reduction in e_{rms}. Also note that the slopes in Eq. (24) are larger for the Lake Washington dataset implying a more rapid increase in z_0 with friction

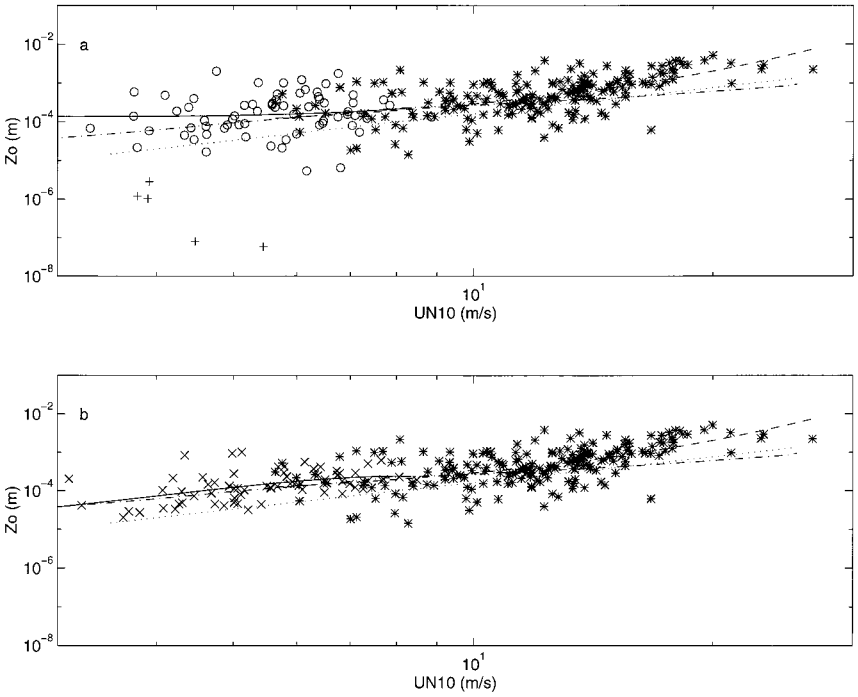

FIG. 7. Surface roughness length z_0 versus wind speed U_{N10}. During HEXMAX atmospheric stratification was mostly near neutral. However, stratification effects on the wind profiles in both datasets were corrected for with the use of Eq. (8) and z/L evaluated from Eq. (2). Note that U_{N10} in plots a and b are slightly different since they were calculated from Eq. 8 using z_0 and $z_{0\zeta}$, respectively. In comparison to Fig. 6, the scatter is larger in all cases. Also, the slope of the fit to the Lake Washington data obtained from fluxes is significantly lower than the others and can not be justified. Again, $z_{0\zeta}$ from waves exhibits a clear and consistent behavior down to the levels of aerodynamically smooth. (For more explanation, see the legend of Fig. 6.) Regression line and e_{rms} for the Lake Washington LW and HEXMAX datasets are (a) LW–flux: $\ln z_0 = 1.19U_{N10} - 9.44$, $e_{\text{rms}} = 1.25$; (b) LW–wave: $\ln z_0 = 3.77U_{N10} - 11.0$, $e_{\text{rms}} = 0.77$; and (a, b) HEXMAX–flux: $\ln z_0 = 1.94U_{N10} - 10.1$, $e_{\text{rms}} = 0.91$.

velocity. This is in accordance with the observations that at a given friction velocity (or wind speed) the drag coefficient, which is proportional to z_0, increases with decreasing fetch (e.g., Geernaert 1990). Agreement between the fits to these datasets and predictions by Liu et al. (1979) is remarkably good. In this range, the model of Liu et al. (1979) uses Kondo's (1975) results obtained from a composite data of field and laboratory measurements. Below this range is a different regime: the aerodynamically smooth flow where z_0 increases again with decreasing u_* as indicated by the curve of Liu et al. (1979). Comparisons above were repeated by replacing the measured u_* with U_{N10} (Fig. 7). Regression line and e_{rms} for the LW and HEXMAX datasets are

$$\begin{aligned} \ln z_0 &= 1.19U_{N10} - 9.44, \\ e_{\text{rms}} &= 1.25 \quad \text{(LW–flux)} \\ \ln z_{0\zeta} &= 3.77U_{N10} - 11.0, \\ e_{\text{rms}} &= 0.77 \quad \text{(LW–wave)} \\ \ln z_0 &= 1.94U_{N10} - 10.1, \\ e_{\text{rms}} &= 0.91 \quad \text{(HEXMAX–flux).} \end{aligned} \tag{25}$$

(The above expressions have been constructed only for the purpose of statistical comparisons and are not suggested for use over water in other sites since they do not include the wave properties.) The first thing to note is that the slope in the expression for the LW–flux is significantly smaller than even that for the HEXMAX–flux. This is contradictory to the findings in Fig. 6 and Eq. (24) as well as to the observations by others. Another point to be noted is the overall increase in e_{rms} [Eqs. (24) and (25)]. These results may seem strange since the wind speed is easier to measure than the friction velocity. However, note that U_{N10} is a quantity adjusted to neutral stratification and a standard height. Stratification effects on the wind profiles in both the Lake Washington and HEXMAX datasets were corrected for with the use of Eq. (8) and z/L evaluated from Eq. (2). It should also be mentioned that U_{N10} for the Lake Washington datasets in plots a and b are slightly different since they were calculated from Eq. (8) using z_0 and $z_{0\zeta}$, respectively. These results show that the stratification adjustments should not be omitted and should be handled with great care, even though they may not seem to be important under the conditions of high winds

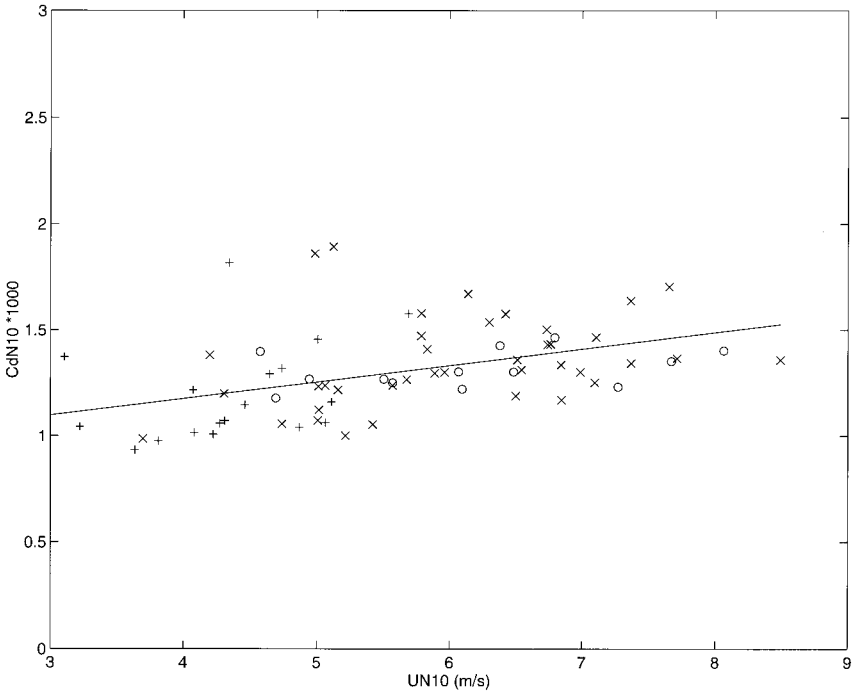

FIG. 8. Neutral drag coefficients obtained at *MSMAST* on Lake Washington. In contrast to Fig. 3, these coefficients were calculated using the surface roughness length $z_{0\zeta}$ determined from the measured wave spectra [Eq. (23)]. Mean value of the drag coefficient is similar to that in Fig. 3, but the scatter in the new neutral drag coefficient is significantly reduced. Regression line and the root-mean-square error, e_{rms}, for this plot are $C_{dN10} = [0.078U_{N10} + 0.87] \times 10^{-3}$, $e_{\text{rms}} = 0.19 \times 10^{-3}$.

and small air–sea temperature differences, as in the case of the HEXMAX dataset.

Since the drag coefficient and U_{N10} are functions of the surface roughness length, these parameters were recalculated using $z_{0\zeta}$, obtained from the measured wave spectra. Comparison of Fig. 8 with its counterpart (Fig. 3) shows that using $z_{0\zeta}$ or z_0 does not affect the mean value of the drag coefficient. However, the scatter in the new neutral drag coefficient in Fig. 8 is significantly reduced. The regression equation and the rms error for the plot in Fig. 8 are

$$C_{DN10} = [0.078U_{N10} + 0.87] \times 10^{-3},$$
$$e_{\text{rms}} = 0.19 \times 10^{-3}. \quad (26)$$

The findings presented above clearly demonstrate that the surface roughness parameter and the neutral drag coefficient determined from the observed wave spectra are much more consistent, that is, show less scatter than those obtained from the measured fluxes. This may be explained as follows. Intermittency in atmospheric turbulence and the low frequency motions in the atmosphere may cause significant sampling variability (Katsaros et al. 1993, 1994b) when observations are conducted at a single point, which in turn may induce large fluctuations in the measured fluxes and in quantities derived from them. These undesired effects can be overcome by spatial averaging of fluxes but such measurements are generally not available. On the other hand, evolution of a wave field involves long time and length scales, thus its response to variations in atmospheric conditions is gradual; that is, a wave field reflects the atmospheric energy input integrated over duration and fetch. For this reason, the parameters obtained from the observations of waves essentially are quantities averaged over both time and space and provide consistent results.

The relationship between the wave spectra and the surface roughness length has been recently examined also by other researchers. For example, Monbaliu (1994) assumed a linear relationship between the dimensionless roughness length and the equilibrium range parameter [Eq. (21)] suggested by Donelan et al. (1985). However, the HEXMAX dataset Monbaliu used indicated a stronger than linear relationship. The latter finding is more appropriate because Monbaliu (1994) considered the Toba (1973) parameter to be constant while it actually varies with wave age (Ataktürk 1991). Using this new relationship he calculated the wind friction velocity from the wave data and compared it to the measured values. The agreement between the two values was within 10% of each other. Juszko et al. (1995) inferred the wind stress from the wave slope spectra using the Phil-

lips (1985) wave model with a constant equilibrium range parameter. They compared these values with the wind stress determined by the dissipation technique and found good agreement. They also noted that the relationships between the dimensionless roughness length and the wave age suggested by Donelan (1990) could describe their data from the Gulf of Alaska only for the young waves and not the fetch-unlimited old waves. Considering that wind stress measurements by the dissipation technique may be in significant error in the presence of swell (Donelan et al. 1997), which existed throughout their experiment, their conclusion on the Donelan (1990) formulation may be questionable. Perrie and Toulany (1995) also derived a relationship between the wind stress and the wave spectral parameters. However, verification of this equation by using field data has not been completed yet.

Deviation of the temporally averaged fluxes from spatial averages increases with lack of horizontal homogeneity and stationarity. This is illustrated in Fig. 9, corresponding to a measurement period of 2 h when the winds over Lake Washington showed the most dramatic variations in speed among the datasets considered (plot a). During this period, the atmospheric stratification was slightly unstable ($z/l = -0.2$, approximately) and light precipitation was observed in the interval between 60 and 70 min. Note that in plot b, C_{DN10} obtained from Eq. (20) and from the observed wave spectra are in good agreement, but C_{DN10} obtained from the measurements of the atmospheric turbulence during this particular period shows significant scatter without any discernible relation to U_{N10}.

With wind speed, duration, and fetch a wave spectrum grows toward lower frequencies by weakly nonlinear wave–wave interactions (Hasselmann 1962). This is a slow process. Thus, ζ being related to the total area under the spectral curve also varies gradually. On the other hand, the portion of the wave spectrum just above the spectral peak is sensitive to changes in the atmospheric input (Donelan et al. 1985; Toba et al. 1988). This is due to rapid growth (decay) of the higher harmonics of the dominant waves during suddenly increasing (decreasing) winds. Since α is determined from a spectral band that includes the first two harmonics, it responds to changing winds quickly. Hence, in Fig. 9c it is seen that C_{DN10} determined from ζ and α closely follows the variations in U_{N10} as does C_{DN10} calculated from the linear fit to all flux data [Fig. 3a, Eq. (20)]. On the other hand, a careful look at plot c also shows that the time series of C_{DN10} from turbulent fluxes reflects a mirror image of U_{N10} shown in plot a. We attribute this behavior to the presence of large-scale motions in the planetary boundary layer and their influence on fluxes in the surface layer. Also note that despite the large scatter in C_{DN10} obtained from turbulent fluxes, there is good agreement between its cumulative means and the results obtained from Eq. (20) and from the measured wave spectra (plot c). This behavior is in accordance with the ergodicity principle that stationarity is achieved over a long enough averaging time such that a time average is equivalent to a space average.

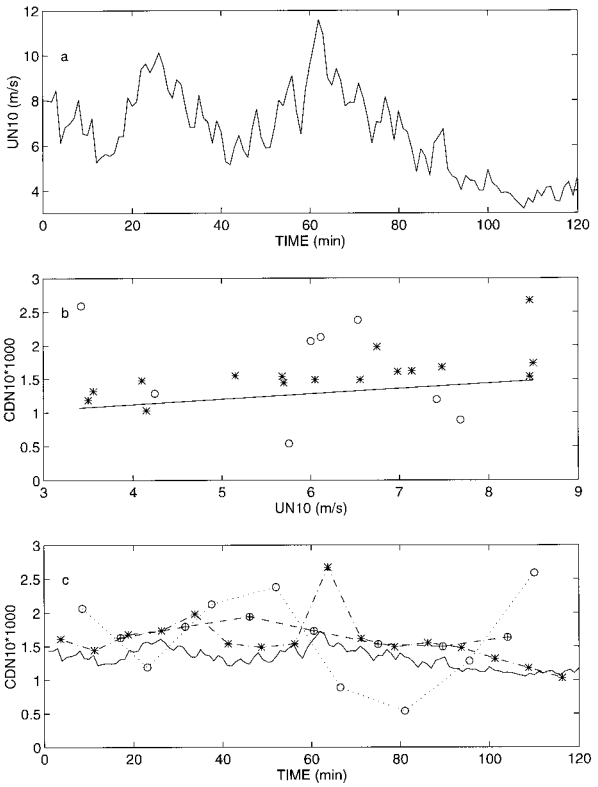

FIG. 9. Plots showing (a) time series of gusty winds (U_{N10}) during a period of 2 h; (b) neutral drag coefficient C_{DN10}, obtained from fluxes (○) and wave spectra (*) versus U_{N10}; and, (c) time series of C_{DN10} calculated from overall statistical results [Eq. (20), solid line], from the measured fluxes (○ and dotted line) and its cumulative mean (⊕ and dashed line) and from the observed wave spectra (* and dash-dotted line). Precipitation was observed between 60 and 70 minutes. C_{DN10} from Eq. (20) from wave spectra and from the cumulative means of the results of turbulent fluxes are in good agreement. Enhanced scatter in C_{DN10} from turbulent fluxes (plot b) in this case study was attributed to the large-scale motions in the planetary boundary layer and their influence on fluxes in the surface layer. This may also be noted in the time series of C_{DN10} from turbulent fluxes (plot c), which is a mirror image of U_{N10} shown in plot a.

Results of the study presented here demonstrate that some air–sea interaction processes near the interface may be investigated through measurements of atmospheric turbulence as well as through observations of the surface wind waves. It is also shown that the latter may prove useful, in particular when the events are transitional. In such cases, the underlying assumptions of the eddy correlation method, that is, horizontal homogeneity and stationarity, may be violated. An extreme example is the frontal zones where studies of the air–sea exchanges are of great importance but the eddy correlation technique is not applicable. The approach used in this study may provide an alternative technique for studying such events. However, this would require better understanding of several processes such as interactions

among wind, wind waves, and swell with different and varying directions of propagations and the partitioning of the atmospheric energy input between waves, currents, and turbulence in the oceanic mixed layer.

5. Summary and conclusions

In this study, air–sea exchange of momentum is investigated through direct measurements conducted at Lake Washington in the range of wind speeds from 2.5 to 9 m s^{-1}. In particular, attention is focused on relating the surface roughness length to some measurable parameters of the surface wind waves. Conclusions drawn from the analyses of the collected data are summarized below.

Dependence of the momentum flux measured at this site on wind speed is generally in accordance both in magnitude and behavior with those from other studies conducted over coastal waters at higher wind speeds. The findings show that the drag coefficient increases with increasing wind speed. Also, the scatter in experimental results becomes larger as the wind speed decreases and the atmospheric stability deviates from neutral stratification.

Surface roughness length being a direct function of the neutral drag coefficient is a key parameter in formulation of the air–sea exchange processes. It is also the quantity most severely affected by scatter in atmospheric turbulence measurements. In an effort to overcome this difficulty, a method to estimate the surface roughness length from the observations of the wind waves was devised. Particular variables relevant to this method are the equilibrium range parameter and the rms wave height, which are readily obtainable from wave height spectra. The improvements achieved by using this approach are consistent with the idea that the water waves have a long memory so that they reflect the atmospheric input integrated over duration and fetch. Thus, its locally observed parameters essentially are quantities averaged over both time and space that are more consistent than those averaged over time only, as is the case with the atmospheric turbulence measurements conducted at a point.

Finally, the analyses of the measured fluxes and the wind waves show that the magnitude of the equilibrium range parameter at Lake Washington was significantly smaller than that predicted by other studies. This observed difference in the growth of wind waves is related to the differences in the basin geometries. Similar effects are expected in other lakes and coastal regions. We note that, since the equilibrium range parameter is site dependent, the method of estimating the surface roughness from wave spectra must be empirically calibrated for a particular location.

Acknowledgments. We thank Ralph Monis, Robert Sunderland, and Noel Cheney for their help with the operation and maintenance of the station. We also thank Hans Hersbach of the Royal Netherlands Meteorological Institute for running the WAM model for the Lake Washington parameters. Work reported in this article was supported by the National Aeronautics and Space Administration under Grant NAGW-1322 and by the National Science Foundation under Grant ATM-9024698.

REFERENCES

Ataktürk, S. S., 1984: Intrinsic frequency spectra of small scale wave amplitude measured in a lake. M.S. thesis, Dept. of Atmospheric Sciences, University of Washington, 96 pp. [Available from Dept. of Atmospheric Sciences, University of Washington, Seattle, WA 98195.]

——, 1991: Characterization of roughness elements on a water surface. Ph.D. dissertation, University of Washington, 196 pp.

——, and K. B. Katsaros, 1987: Intrinsic frequency spectra of short gravity–capillary waves obtained from temporal measurements of wave height on a lake. *J. Geophys. Res.,* **92,** 5131–5141.

——, and ——, 1989: The K-Gill: A twin propeller–vane anemometer for measurements of atmospheric turbulence. *J. Atmos. Oceanic Technol.,* **6,** 509–515.

Banner, M. L., 1990: The influence of wave breaking on the surface pressure distribution in the wind–wave interactions. *J. Fluid Mech.,* **211,** 463–495.

——, and O. M. Phillips, 1974: On the incipient breaking of small scale waves. *J. Fluid Mech.,* **65,** 647–656.

Blanc, T. V., 1985: Variation of bulk-derived surface flux, stability, and surface roughness results due to the use of different transfer coefficient schemes. *J. Phys. Oceanogr.,* **15,** 650–669.

——, 1987: Accuracy of bulk-method-determined flux, stability, and sea surface roughness. *J. Geophys. Res.,* **92,** 3867–3876.

Brown, R. A., and W. T. Liu, 1982: An operational large-scale marine planetary boundary layer model. *J. Appl. Meteor.,* **21,** 261–269.

Busch, N. E., 1973: On the mechanics of atmospheric turbulence. *Workshop on Micrometeorology,* D. A. Haugen, Ed., Amer. Meteor. Soc., 1–65.

Businger, J. A., 1973: Turbulent transfer in the atmospheric surface layer. *Workshop in Micrometeorology,* D. A. Haugen, Ed., Amer. Meteor. Soc., 67–100.

——, J. C. Wyngaard, Y. Izumi, and E. F. Bradley, 1971: Flux–profile relationships in the atmospheric surface layer. *J. Atmos. Sci.,* **28,** 181–189.

Byrne, H. M., 1982: The variation of the drag coefficient in the marine surface layer due to temporal and spatial variations in the wind sea state. Ph.D. dissertation, University of Washington.

Charnock, H., 1955: Wind stress on a water surface. *Quart. J. Roy. Meteor. Soc.,* **81,** 639–640.

——, 1958: A note on empirical wind-wave formulae. *Quart. J. Roy. Meteor. Soc.,* **84,** 443–447.

DeCosmo, J., 1991: Air–sea exchange of momentum, heat, and water vapor over whitecap sea states. Ph.D. dissertation, University of Washington, 213 pp.

——, K. B. Katsaros, S. D. Smith, R. J. Anderson, W. A. Oost, K. Bumke, and H. M. Chadwick, 1996: Air–sea exchange of sensible heat and water vapor: The Humidity Exchange Over the Sea (HEXOS) results. *J. Geophys. Res.,* **101,** 12 001–12 016.

Dobson, F. W., and J. A. Elliott, 1978: Wave-pressure correlation measurements over growing sea waves with a wave follower and fixed-height pressure sensors. *Turbulent Fluxes Through the Sea Surface, Wave Dynamics, and Prediction,* A. Favre and K. Hasselmann, Eds., Plenum Press, 421–432.

Donelan, M. A., 1982: The dependence of the aerodynamic drag coefficient on wave parameters. *First Int. Conf. on Meteorology and Air–Sea Interaction of the Coastal Zone,* Boston, MA, Amer. Meteor. Soc., 381–387.

——, 1990: Air–sea interaction. *The Sea.* Vol. 9a, B. LeMéhauté and D. M. Hanes, Eds., J. Wiley and Sons, 239–292.
——, J. Hamilton, and W. H. Hui, 1985: Directional spectra of wind-generated waves. *Philos. Trans. Roy. Soc. London, Series A,* **315,** 509–562.
——, F. W. Dobson, S. D. Smith, and R. J. Anderson, 1993: On the dependence of sea surface roughness on wave development. *J. Phys. Oceanogr.,* **23,** 2143–2149.
——, W. M. Drennan, and K. B. Katsaros, 1997: The air–sea momentum flux in conditions of wind sea and swell. *J. Phys. Oceanogr.,* **27,** 2087–2099.
Dyer, A. J., 1974: A review of flux-profile relationships. *Bound.-Layer Meteor.,* **7,** 363–372.
Garratt, J. R., 1977: Review of drag coefficients over oceans and continents. *Mon. Wea. Rev.,* **105,** 915–928.
Geernaert, G. L., 1990: Bulk parameterizations for the wind stress and heat fluxes. *Surface Waves and Fluxes: Volume 1—Current Theory,* G. L. Geernaert and W. J. Plant, Eds., Kluwer Academic, 91–172.
——, and K. B. Katsaros, 1986: Incorporation of stratification effects on the oceanic roughness length in the derivation of the neutral drag coefficient. *J. Phys. Oceanogr.,* **16,** 1580–1584.
——, ——, and K. Richter, 1986: Variation of the drag coefficient and its dependence on sea state. *J. Geophys. Res.,* **91,** 7667–7679.
——, S. E. Larsen, and F. Hansen, 1987: Measurements of the wind stress, heat flux, and turbulence intensity during storm conditions over the North Sea. *J. Geophys. Res.,* **92,** 13 127–13 139.
Gill, G. C., 1975: Development and use of the UVW anemometer. *Bound.-Layer Meteor.,* **8,** 475–495.
Hasse, L., M. Grünewald, J. Wucknitz, M. Dunckel, and D. Schriever, 1978: Profile derived turbulent fluxes in the surface layer under disturbed and undisturbed conditions during GATE. *Meteor-Forschungsergebnisse,* **13,** 24–40.
Hasselmann, K., 1960: Grundgleichungen der Seegangsvorhersage. *Schiffstechnik,* **7,** 191–195.
——, 1962: On the nonlinear energy transfer in a gravity-wave spectrum: Part 1. General theory. *J. Fluid Mech.,* **12,** 481–500.
——, K. Hasselmann, J. H. Allender, and T. P. Barnett, 1985: Computations and parameterizations of the nonlinear energy transfer in a gravity-wave spectrum: Part 2. Parameterizations of the nonlinear energy transfer for application in wave models. *J. Phys. Oceanogr.,* **15,** 1378–1391.
——, J. Bösenberg, M. Dunckel, K. Richter, M. Grünewald, and H. Carlson, 1986: Measurements of wave-induced pressure over surface gravity waves. *Wave Dynamics and Radio Probing of the Ocean Surface,* O. M. Phillips and K. Hasselmann, Eds., Plenum Press, 353–368.
Hicks, B. B., 1972: Propeller anemometers as sensors of atmospheric turbulence. *Bound.-Layer Meteor.,* **3,** 214–228.
Holmes, R. M., G. C. Gill, and H. W. Carson, 1964: A propeller-type vertical anemometer. *J. Appl. Meteor.,* **3,** 802–804.
Hsiao, S. V., and O. H. Shemdin, 1983: Measurements of wind velocity and pressure with a wave follower during MARSEN. *J. Geophys. Res.,* **88,** 9841–9849.
Hsu, S. A., 1974: A dynamic roughness equation and its application to wind stress determination at the air–sea interface. *J. Phys. Oceanogr.,* **4,** 116–120.
——, 1986: A mechanism for the increase of wind stress (drag) coefficient with wind speed over water waves: A parametric model. *J. Phys. Oceanogr.,* **16,** 144–150.
Huang, N. E., L. F. Bliven, S. R. Long, and P. S. DeLeonibus, 1986: A study of the relationship among wind speed, sea state, and the drag coefficient for a developing wave field. *J. Geophys. Res.,* **91,** 7733–7742.
Janssen, P. A. E. M., 1989: Wave-induced stress and the drag of air flow over sea waves. *J. Phys. Oceanogr.,* **19,** 745–754.
——, 1991: Quasi-linear theory of wind–wave generation applied to wave forecasting. *J. Phys. Oceanogr.,* **21,** 1631–1642.
——, 1992: Experimental evidence of the effect of surface waves on the airflow. *J. Phys. Oceanogr.,* **22,** 1600–1604.
Jenkins, A. D., 1992: A quasi-linear eddy-viscosity model for the flux of energy and momentum to wind waves using conservation–law equations in a curvilinear coordinate system. *J. Phys. Oceanogr.,* **22,** 843–858.
Juszko, B.-A., R. F. Marsden, and S. R. Waddel, 1995: Wind stress from wave slopes using Phillips equilibrium theory. *J. Phys. Oceanogr.,* **25,** 185–203.
Kahma, K. K., and M. A. Donelan, 1988: A laboratory study of the minimum wind speed for wind wave generation. *J. Fluid Mech.,* **192,** 339–364.
——, and H. Pettersson, 1994: Wave growth in a narrow fetch geometry. *Global Atmos. Ocean Sys.,* **2,** 253–263.
Katsaros, K. B., H. Gucinski, S. S. Ataktürk, and R. Pincus, 1989: Effects of reduced surface tension on short waves at low wind speeds in a fresh water lake. *Radar Scattering from Modulated Wind Waves,* G. J. Komen and W. A. Oost, Eds., Kluwer Academic, 61–74.
——, M. A. Donelan, and W. M. Drennan, 1993: Flux measurements from a SWATH ship in SWADE. *J. Mar. Sys.,* **4,** 117–132.
——, J. M. DeCosmo, R. J. Lind, R. J. Anderson, S. D. Smith, G. Kraan, W. Oost, K. Uhlig, P. G. Mestayer, S. E. Larsen, M. H. Smith and G. deLeeuw, 1994a: Measurements of humidity and temperature in the marine environment during the HEXOS main experiment. *J. Atmos. Oceanic Technol.,* **11,** 964–981.
——, M. A. Donelan, W. M. Drennan, and K. M. Howard, 1994b: Surface fluxes and their relation to planetary boundary layer structure. *The Air–Sea Interface,* M. A. Donelan, W. H. Hui, and W. J. Plant, Eds., RSMAS, University of Miami, 483–488.
Kawai, S., K. Okuda, and Y. Toba, 1977: Field data support of three-seconds power law and spectral form for growing wind waves. *J. Oceanogr. Soc. Japan,* **33,** 137–150.
Kitaigorodskii, S. A., 1968: On the calculation of the aerodynamic roughness of the sea surface. *Izv. Atmos. Ocean. Phys.,* **4.**
——, 1970: *The Physics of Air–Sea Interaction.* (English ed.) A. Baruch, Translator, P. Greenberg, Ed., Israel Program for Scientific Translations, 237 pp.
——, and Y. A. Volkov, 1965: On the roughness parameter of the sea surface and the calculation of the momentum flux in the near water layer of the atmosphere. *Izv. Atmos. Ocean Phys.,* **1,** 973–988.
Komen, G. J., L. Cavaleri, M. Donelan, K. Hasselmann, and P. A. E. M. Janssen, 1995: *Dynamics and Modelling of Ocean Waves.* Cambridge University Press, 532 pp.
Kondo, J., 1975: Air–sea bulk transfer coefficients in diabatic conditions. *Bound.-Layer Meteor.,* **9,** 91–112.
——, Y. Fujinawa, and G. Naito, 1973: High-frequency components of ocean waves and their relation to the aerodynamic roughness. *J. Phys. Oceanogr.,* **3,** 197–202.
Large, W. G., and S. Pond, 1981: Open ocean momentum flux measurements in moderate to strong winds. *J. Phys. Oceanogr.,* **11,** 324–336.
——, and ——, 1982: Sensible and latent heat flux measurements over the ocean. *J. Phys. Oceanogr.,* **12,** 464–482.
Liu, W. T., K. B. Katsaros, and J. A. Businger, 1979: Bulk parameterizations of air–sea exchanges of heat and water vapor including the molecular constraints at the interface. *J. Atmos. Sci.,* **36,** 1722–1735.
——, ——, and M. A. Weissman, 1982: Dynamic response of thin-wire wave gauges. *J. Geophys. Res.,* **87,** 5686–5698.
Maat, N., C. Kraan, and W. A. Oost, 1991: The roughness of wind waves. *Bound.-Layer Meteor.,* **54,** 89–103.
Masuda, A., and T. Kusaba, 1987: On the local equilibrium of winds and wind-waves in relation to surface drag. *J. Oceangr. Soc. Japan,* **43,** 28–36.
Merzi, N., and W. H. Graf, 1985: Evaluation of the drag coefficient considering the effects of mobility of the surface elements. *Ann. Geophys.,* **3,** 473–478.

Miche, M., 1951: Action of the swell. *Ann. Ponts Chaussees,* **121,** 285–319.

Monbaliu, J., 1994: On the use of Donelan wave spectral parameter as a measure for the roughness of wind waves. *Bound.-Layer Meteor.,* **67,** 277–291.

Monin, A. S., and A. M. Obukhov, 1954: Basic laws of turbulent mixing in the ground layer of the atmosphere. *Tr. Akad. Nauk SSSR Geofiz. Inst.,* **151,** 163–187.

——, and A. M. Yaglom, 1971: *Statistical Fluid Mechanics. Vol 1: Mechanics of Turbulence,* The MIT Press, 769 pp.

Obukhov, A. M., 1946: Turbulence in an atmosphere with a non-uniform temperature. *Tr. Akad. Nauk SSSR Inst. Teoret. Geofiz.,* **1** (Transl. in *Bound.-Layer Meteor.,* **2,** 7–29).

Panofsky, H. A., and J. A. Dutton, 1984: *Atmospheric Turbulence: Models and Methods for Engineering Applications.* J. Wiley Intersciences, 397 pp.

Paulson, C. A., 1970. The mathematical representation of wind speed and temperature profiles in the unstable atmospheric surface layer. *J. Appl. Meteor.,* **9,** 857–861.

Perrie, W., and B. Toulany, 1990: Fetch relations for wind-generated waves as a function of wind stress scaling. *J. Phys. Oceanogr.,* **20,** 1666–1681.

——, and ——, 1995: Relating friction velocity to spectral wave parameters. *J. Phys. Oceanogr.,* **25,** 266–279.

Phillips, O. M., 1977: *The Dynamics of the Upper Ocean.* Cambridge University Press, 336 pp.

Plant, W. J., 1990: Bragg scattering of electromagnetic waves from the air/sea interface. *Surface Waves and Fluxes*: Vol. II *Remote Sensing,* G. L. Geernaert and W. J. Plant, Eds., Kluwer Academic 41–108.

Schlichting, H., 1968: *Boundary-Layer Theory.* 6th ed. McGraw-Hill, 747 pp.

Shaw, W. J., and J. E. Tillman, 1980: The effect of and correction for different wet-bulb and dry-bulb response in thermocouple psychrometry. *J. Appl. Meteor.,* **19,** 90–97.

Smith, S. D., 1980: Wind stress and heat flux over the ocean in gale force winds. *J. Phys. Oceanogr.,* **10,** 709–726.

——, 1988: Coefficients for sea surface wind stress, heat flux, and wind profiles as a function of wind speed and temperature. *J. Geophys. Res.,* **93,** 15 467–15 472.

——, R. J. Anderson, W. A. Oost, C. Kraan, N. Maat, J. DeCosmo, K. B. Katsaros, K. L. Davidson, K. Bumke, L. Hasse and H. M. Chadwick, 1992: Sea surface wind stress and drag coefficients: The HEXOS results. *Bound.-Layer Meteor.,* **60,** 109–142.

Snyder, R. L., F. W. Dobson, J. A. Elliott, and R. B. Long, 1981: Array measurements of atmospheric pressure fluctuations above surface gravity waves. *J. Fluid Mech.,* **102,** 1–59.

Stewart, R. W., 1974: The air–sea momentum exchange. *Bound.-Layer Meteor.,* **6,** 151–167.

Tennekes, H., and J. L. Lumley, 1972: *A First Course in Turbulence.* The MIT Press, 300 pp.

Toba, Y., 1979: Study on wind waves as a strongly nonlinear phenomenon. *Twelfth Symp. on Naval Hydrodynamics,* Washington, DC, 529–540.

——, and M. Koga, 1986: A parameter describing overall conditions of wave breaking, whitecapping, sea-spray production, and wind stress. *Oceanic Whitecaps,* E. C. Monahan and G. Mac Niocaill, Eds., D. Reidel, 37–47.

——, K. Okada, and I. S. F. Jones, 1988: The response of wind–wave spectra to changing winds. Part I: Increasing winds. *J. Phys. Oceanogr.,* **18,** 1231–1240.

——, N. Iida, H. Kawamura, N. Ebuchi, and I. S. F. Jones, 1990: Wave dependence of sea-surface wind stress. *J. Phys. Oceanogr.,* **20,** 705–721.

Wu, J., 1980: Wind stress coefficients over the sea surface near neutral conditions—A revisit. *J. Phys. Oceanogr.,* **10,** 727–740.

——, 1988: On nondimensional correlation between roughness length and wind-friction velocity. *J. Oceanogr. Soc. Japan,* **44,** 254–260.

Zhang, S. F., 1988: A critical evaluation of the von Kármán constant from a new atmospheric surface layer experiment. Ph.D. dissertation, University of Washington.

——, S. P. Oncley, and J. A. Businger, 1988: A critical evaluation of the von Karman constant from a new atmospheric surface layer experiment. Preprints, *Eighth Symp. on Turbulence and Diffusion,* San Diego, CA, Amer. Meteor. Soc., 148–150.